Chloroplast Genome Comparison and Evolution Analysis of Dendrobium (Orchidaceae) among Multiple Photosynthetic Pathways

Yajun Lin , Shibao Zhang , Jun Duan , Jingshan Shi , Ding-Kun Liu , Siren Lan , Zhong-Jian Liu , Ming-He Li *

Posted Date: 29 December 2023

doi: 10.20944/preprints202312.2150.v1

Keywords: Dendrobium; Orchidaceae; Chloroplast genome; CAM evolution

Article

Chloroplast Genome Comparison and Evolution Analysis of *Dendrobium* (Orchidaceae) Among Multiple Photosynthetic Pathways

Yajun Lin [1], Shibao Zhang [2], Jun Duan [3], Jingshan Shi [4], Ding-Kun Liu [1], Siren Lan [1], Zhong-Jian Liu [1] and Ming-He Li [1,*]

[1] Key Laboratory of National Forestry and Grassland Administration for Orchid Conservation and Utilization, College of Landscape Architecture and Art, Fujian Agriculture and Forestry University, Fuzhou 350002, China
[2] Key Laboratory of Economic Plants and Biotechnology, Kunming Institute of Botany, Chinese Academy of Sciences, Kunming 650201, China
[3] South China National Botanical Garden, Guangzhou 510650, China
[4] Key Laboratory of Basic Pharmacology of Ministry of Education and Joint International Research Laboratory of Ethnomedicine of Ministry of Education, Zunyi Medical University, Zunyi Guizhou 563099, China
* Correspondence: fjalmh@fafu.edu.cn (M.-H.L.)

Abstract: *Dendrobium* Sw have multiple photosynthetic pathways but due to the lack of identification, the influence of CAM pathway on the plastid genomic evolution of *Dendrobium* and the origin of CAM pathway are still poorly understood. In this study, based on the results of $\delta^{13}C$, net photosynthetic rates (Pn) and titratable acid value, we identified *Dendrobium* species into three photosynthetic pathways. Then the chloroplast whole genome characteristics of 10 *Dendrobium* species were analyzed with next-generation sequencing technology. The quadripartite-structure plastomes ranged from 151,673 bp to 160,375 bp and included 127 to 132 genes. Five noncoding mutational hotspots (*rbcL-accD*, *atpB-rbcL*, *rbcL*, *trnL*^{UAA}, *accD*, Pi > 0.10) were identified. A total of 41–60 SSRs were recognized, the average trinucleotide content was only about 4%, which is probably due to a more conserved SSR. Among multiple photosynthetic pathways, the apparent differences in IR junctions of SSC/IRB junctions (JSBs) were measured within chloroplast genomes, and the chloroplast genome size of constitutive CAM plants is shorter because of their *ndh* gene loss or pseudogenization, and this phenomenon accounts for a decreasing proportion of constitutive CAM, facultative CAM, and obligate C_3 plants, so that the loss of the *ndh* gene may be speculated to be closely related to the CAM pathway. Phylogenetic analyses showed that there are multiple independent CAM origins in selected *Dendrobium* species, and the ancestral *Dendrobium* plastome possessed full ORFs for all *ndh* genes. The study aims to clarify the chloroplast genomic features of different photosynthetic pathways, enrich the genomic data of CAM plants, and provide genetic information from different perspectives for further systematic study of *Dendrobium*.

Keywords: *Dendrobium*; Orchidaceae; chloroplast genome; CAM evolution

1. Introduction

Crassulacean acid metabolism (CAM) is an important photosynthetic pathway in addition to C_3 and C_4, which often exists in species with CO_2 or water-limited environments, such as aquatic habitats, tropical rainforests and arid regions [1], so plants with CAM pathway typically have higher water use efficiency and greater drought tolerance. Recent studies have revealed the multiple independent origins of the CAM pathway, which have existed in 18,000 species among 400 genera of 40 families minimally [2-4], accounting for about 6% [5-7] to 7% [8,9] vascular plants. Of which about 10% Orchidaceae exercise CAM pathway [10], with the most CAM species diversity. *Dendrobium* Sw. is the second largest genus of Orchidaceae [11], containing rich CAM resources. However,

 doi:10.20944/preprints202312.2150.v1

Dendrobium CAM plants identification is mainly based on the determination of carbon isotope($\delta^{13}C$) value [12-14], which cannot distinguish C_3 plants with CAM pathway. Because some C_3 plants subjected to external influences (e.g., drought stress) also activate the CAM pathway, such plants were defined as facultative CAM plants [2,15,16]. So far, studies on the identification of *Dendrobium* facultative CAM plants have lagged relatively behind, only a few species have been reported: *D. officinale, D. nobile, D. hercoglossum, D. moniliforme, D. heterocarpum, D. chrysotoxum, D. wardianum, D. findlayanum* and two cultivars (*D. nobile* 'V1', *D. nobile* 'V4') were identified as facultative CAM under drought stress [17-25]. Previous studies have shown that the CAM pathway has independently evolved at least eight times in *Dendrobium* [14]. However, due to the lack of identification of different photosynthetic pathways, especially the facultative CAM, the number of CAM origins is more abundant than expected, we still know little about the resources and origins of *Dendrobium* CAM.

Chloroplast, the power factories for plant growth and development, is the most critical organelles for plant photosynthesis. In recent years, 153 complete chloroplast genomes of *Dendrobium* have been published [26], research on the them have revealed that: (i) independent absence of *ndh* genes in diferent *Dendrobium* lineage, e.g. Niu et al. [27] compared 30 *Dendrobium* plastids and found that *ndhC, I* and *K* were lost in all species, *ndhA* and *H* were also lost and *ndhF* was pseudogenized in *D. huoshanense* and *D. moniliforme*. (ii) the evolution rates of the non-coding regions were diversifed. For instance, different *Dendrobium* species combinations showed inconsistent patterns in the top10 mutational hotspots [27,28]. However, there is little research on whether these differences are related to the presence of CAM pathways: Xue et al. [25] compared the chloroplast genomes of *Dendrobium* with multiple photosynthetic pathways and concluded that different photosynthetic pathways led to the non-proportional evolution of the chloroplast genomes of *Dendrobium*. But there remains a lack of information about the relationship between the evolution of the CAM pathway and the variation among *Dendrobium* chloroplast genomes.

Due to the lack of identification of different photosynthetic pathways, there are few studies on the influence of CAM pathway on the genomic evolution of *Dendrobium* plasmid, and little is known about the origin of CAM pathway. Therefore, in this study, we analyzed the chloroplast genomes of 10 *Dendrobium* species, including whole-genome sequencing of six species and five previously published genome sequences in NCBI. Different photosynthetic pathways were identified using $\delta^{13}C$ values, net photosynthetic rates (Pn) and titratable acidity values. The plastid structure, mutation hotspots, sequence differences and repeat regions were characterized, variable sites were identified, and the phylogenetic tree was constructed. Then we compared the relationship between different photosynthetic pathways and chloroplast genome variation in *Dendrobium.* The aim of this study was to clarify the chloroplast genome characteristics, enrich CAM plants genome data and provide genetic information from different perspectives for further systematic study of *Dendrobium*.

2. Results

2.1. Identification of Multiple Photosynthetic Pathways in Dendrobium

The photosynthetic pathways of 10 *Dendrobium* species were identified in this study. Leaf $\delta^{13}C$ values of them ranged from -30.0‰ (*D. capituliflorum*) to -13.6‰ (*D. delacourii*). According to previous studies [29], -20‰ was used as a cutoff to distinguish C_3 plants from constitutive CAM plants, therefore, *D. capituliflorum, D. fimbriatum, D. jiajiangense, D. aphrodite, D. cumulatum, D. fanjingshanense, D. stuposum* were identified as C_3 plants preliminarily; *D. aphyllum*, *D. delacourii* and *D. parishii* were identified as constitutive CAM plants (Table 1).

Combined with the net photosynthetic rates (Pn) curve, the obligatory C_3 and facultative CAM in C_3 plants were distinguished. The Pn of *D. aphyllum, D. delacourii* and *D. parishii* were negative during the day and positive at night, which showed a very significant trend at night, further verified that they were constitutive CAM plants. Among the C_3 plants（$\delta^{13}C$<-20‰）, *D. cumulatum* and *D. stuposum* had Pn expanded Zero during both day and night, can be determined as facultative CAM. The rest of C_3 plants, their Pn were positive during the day and negative at night, with a non-significant trend at night, which is exact opposite of the constitutive CAM plants (Figure 1).

Preprints (www.preprints.org) | NOT PEER-REVIEWED | Posted: 29 December 2023 doi:10.20944/preprints202312.2150.v1

Further combined with titratable acid values，all three constitutive CAM species($\delta^{13}C \geq -20‰$) had significant day-night titratable acid differences. C_3 plants($\delta^{13}C < -20‰$) of *D. capituliflorum*, *D. fimbriatum* and *D. jiajiangense* had non-significant day-night titratable acid differences, which were determined to be obligate C_3 plants, while *D. aphrodite*, *D. cumulatum*, *D. fanjingshanense* and *D. stuposum* showed significant differences, which clearly were facultative CAM plants (Table 1).

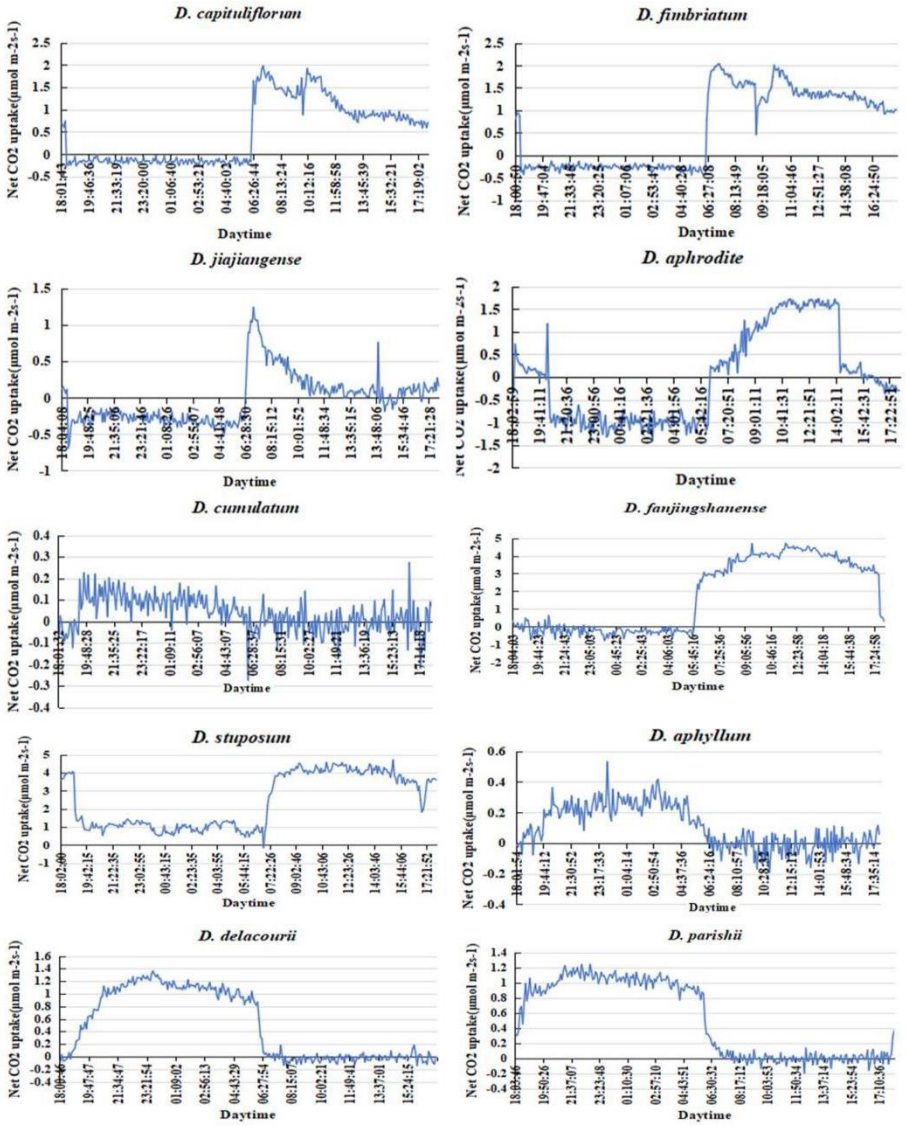

Figure 1. Diurnal CO_2 exchange rate of the 10 *Dendrobium* species.

Table 1. Photosynthetic characteristics of 10 *Dendrobium* species.

Scientific Name	$\delta^{13}C$ (‰)	CO_2 Absorption at Night	Titrable Acid Value/ (mmol kg^{-1})		ΔH^+ (mmol kg^{-1})	Type
			Day	Night	Day-Night	
D. capituliflorum	-30.0	non-significant	12±0.0	12±0.2	0	obligate C_3
D. fimbriatum	-29.4	non-significant	12±0.0	15±0.9	-3	obligate C_3
D. jiajiangense	-29.2	non-significant	21±0.9	23±0.9	-2*	obligate C_3
D. aphrodite	-27.7	non-significant	82±0.6	65±1.1	17*	facultative CAM

Preprints (www.preprints.org) | NOT PEER-REVIEWED | Posted: 29 December 2023 doi:10.20944/preprints202312.2150.v1

D. cumulatum	-27.7	significant	59±3.7	30±4.7	29*	facultative CAM
D. fanjingshanense	-29.3	non-significant	117±12.5	60±3.6	57*	facultative CAM
D. stuposum	-27.5	extremely significant	173±14.7	101±9.4	72*	facultative CAM
D. aphyllum	-15.0	extremely significant	36±0.7	10±0.0	26*	constitutive CAM
D. delacourii	-13.6	extremely significant	87±2.0	38±1.3	49*	constitutive CAM
D. parishii	-16.8	extremely significant	26±0.5	16±0.5	10*	constitutive CAM

Note: The significant difference of CO_2 absorption at night, which can be divided into extremely significant, significant and non-significant. The determination criteria are as follows: extremely significant means that CO_2 absorption of more than two thirds of the time at night is positive with a peak; significant means that CO_2 absorption of more than one third of the time at night is positive with no peak; non-significant means that CO_2 absorption of more than one third of the time at night is negative. "*" show titratable acids differ significantly at different time periods.

2.2. Characteristics of the Plastome

The chloroplast genomes of the 10 *Dendrobium* species, all of which showed a typical double-linked tetrad structure, consisted of a small single-copy region (SSC), a large single-copy region (LSC), and two inverted repeat regions (IRa and IRb) (Figure 2).The SSC ranged from 14,328 bp to 18,479 bp for the obligate C_3, from 13,689 bp to 18,650 bp for the facultative CAM, and from 13,550 bp to 14,396 bp for the constitutive CAM; the LSC ranged from 84,763 bp to 87,938 bp for obligate C_3, from 84,990bp to 87,657 bp for the facultative CAM, and from 84,703 bp to 85,647bp for the constitutive CAM; the IRs ranged from 26,291 bp to 27,081 bp for the obligate C_3, from 26,029 bp to 27,107 bp for the facultative CAM, and from 26,026 bp to 27,040 bp for the constitutive CAM (Table 2).

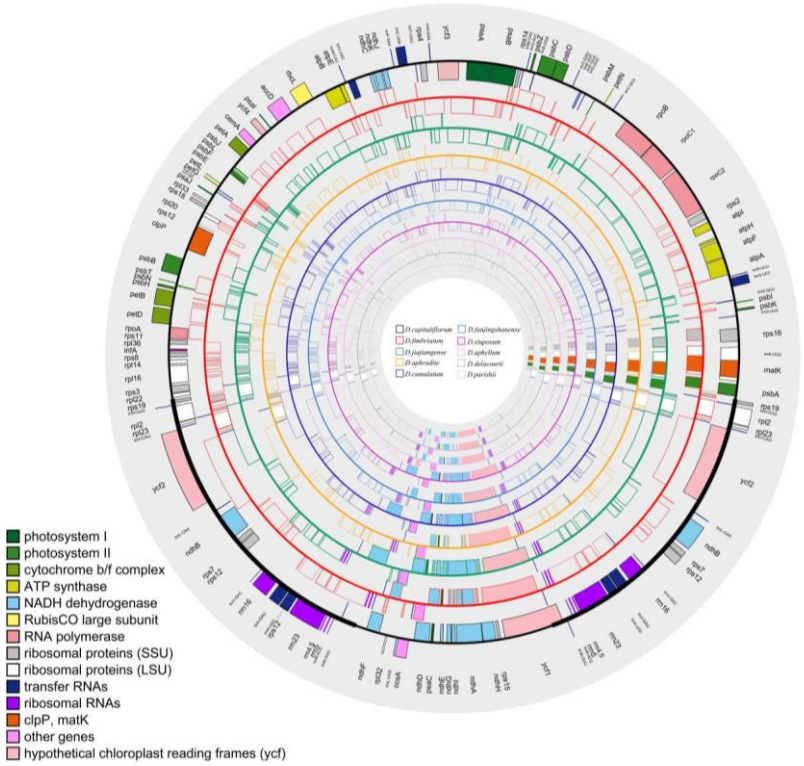

Figure 2. Annotation map of chloroplast genome, 10 *Dendrobium* species are displayed using distinct colors, the constitutive CAM-facultative CAM-obligate C_3 from the inside out.

The genome sizes of obligate C_3 ranged from 151,673 bp to 160,010 bp, and the GC content ranged from 37.2% to 37.6%; facultative CAM plants ranged from 152,108 bp to 160,375 bp, and the GC content ranged from 37.1% to 37.5%; constitutive CAM plants ranged from 151,689 bp to 152,487

 doi:10.20944/preprints202312.2150.v1

bp, and the GC content ranged from 37.5% to 37.6%; the GC content (43.1%-43.5%) in IRs of 10 *Dendrobium* species were higher than that in LSC (34.8%-35.3%) and SSC (30.1%-30.9%) (Table 2).

Table 2. The statistics of plastome characters.

Scientific Name	Chloroplast Genome (bp)	LSC Length/ bp (%)	IR Length/ bp (%)	SSC Length/ bp (%)	GC Content %			
					Total	LSC	IRs	SSC
D. capituliflorum	159,891	87,938 (55.0)	27,069 (16.9)	17,833 (11.2)	37.2	34.9	43.2	30.4
D. fimbriatum	151,673	84,763 (55.9)	26,291 (17.3)	14,328 (9.4)	37.6	35.2	43.4	30.9
D. jiajiangense	160,010	87,369 (54.6)	27,081 (16.9)	18,479 (11.5)	37.2	35.0	43.1	30.4
D. aphrodite	152,687	86,940 (56.9)	26,029 (17.0)	13,689 (9.0)	37.5	35.1	43.4	30.5
D. cumulatum	160,375	87,657 (54.7)	27,034 (16.9)	18,650 (11.6)	37.1	34.8	43.1	30.4
D. fanjingshanense	152,108	84,990 (55.9)	26,302 (17.3)	14,514 (9.5)	37.5	35.1	43.4	30.5
D. stuposum	159,894	87,166 (54.5)	27,107 (17.0)	18,514 (11.6)	37.2	35.0	43.1	30.4
D. aphyllum	152,487	84,857 (55.6)	27,040 (17.7)	13,550 (8.9)	37.5	35.1	43.2	30.1
D. delacourii	152,079	85,647 (56.3)	26,026 (17.1)	14,380 (9.5)	37.7	35.3	43.5	30.9
D. parishii	151,689	84,703 (55.8)	26,295 (17.3)	14,396 (9.5)	37.6	35.2	43.4	30.6

A total of 127-132 genes were encoded (Supplementary FigureS1), and the difference was the number of *ndh* genes. Among the obligate C_3 plants, 11 complete *ndh* genes were present in *D. capituliflorum* and *D. jiajiangense*, while *D. fimbriatum* lost *ndhC, ndhI, ndhK* and was pseudogenticized in *ndhA, ndhF,* and *ndhG;* Among the facultative CAM plants, 11 complete *ndh* genes were present in *D. cumulatum* and *D. stuposum*, while *D .aphrodite* lost *ndhA, ndhF, ndhI* and was pseudogenized with *ndhG* and *ndhH, D. fanjingshanense* lost *ndhC, ndhI, ndhK* and was pseudogenized with *ndhA, ndhF,* and *ndhG*; Among the constitutive CAM plants, 11 complete *ndh* genes were not present, *D. aphyllum* and *D. parishii* lost *ndhC, ndhI, ndhK* and *ndhA, ndhF, ndhG* pseudogenized, *D. delacourii* lost *ndhC, ndhE, ndhF, ndhG, ndhK* and *ndhD, ndhH, ndhI, ndhJ* pseudogenized (Figure 3, Supplementary TableS2).

Preprints (www.preprints.org) | NOT PEER-REVIEWED | Posted: 29 December 2023 doi:10.20944/preprints202312.2150.v1

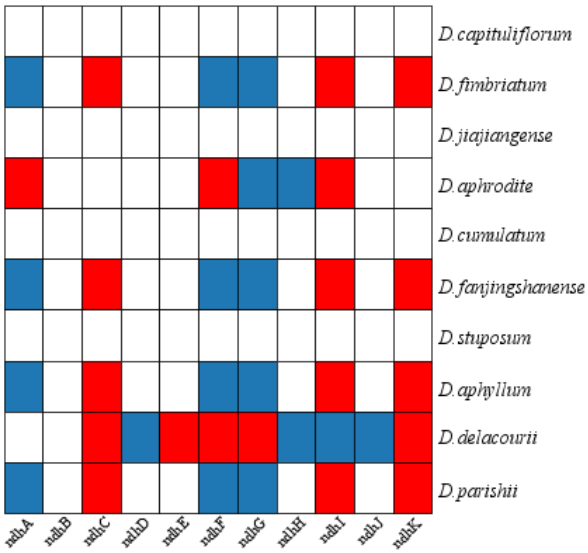

Figure 3. *ndh* gene in *Dendrobium*. Pseudogenization and loss of *ndh* are shown in blue and red, respectively.

2.3. Repeated Analysis

The total number of SSRs ranged from 41 to 60. Mononucleotide, dinucleotide, and tetranucleotide were the nucleotide types common to the 10 *Dendrobium* species; trinucleotide did not appear in *D. delacourii*, pentanucleotide did not appear in *D. fimbriatum, D. jiajiangense, D. aphrodite, D. cumulatum, D. stuposum, D. aphyllum,* and hexanucleotide did not appear in *D. aphrodite, D. fanjingshanense, D. aphrodite* (Figure 4a).

The number of dispersions SSRs of the 10 *Dendrobium* species varied little, and all of them contained four types of repeat sequences, including forward, reverse, palindrome and complementary; the proportion of palindrome was the highest among the four types of repeat sequences, and complementary accounted for the smallest proportion (Figure 4b).

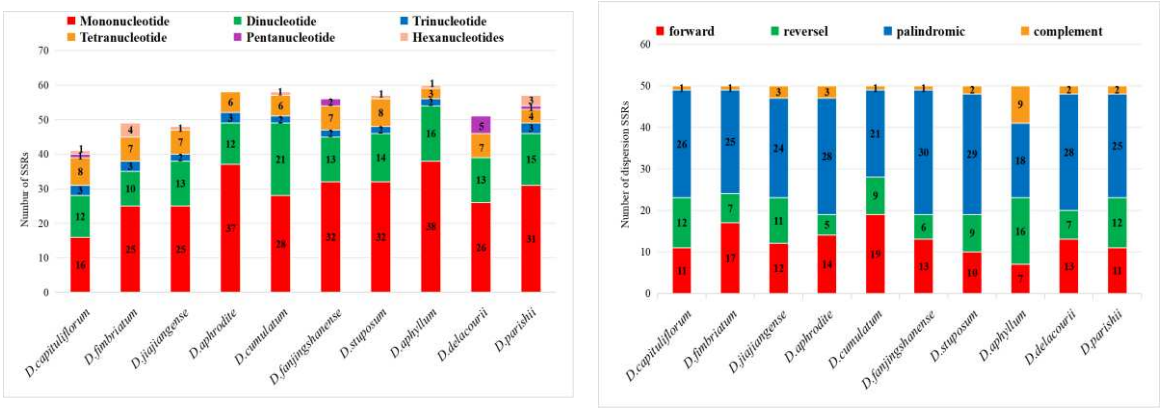

(**a**) (**b**)

Figure 4. Summary of the simple sequence repeats (SSR) across the *Dendrobium* species. (a) Numbur of SSRs; (b) Number of dispersions SSRs.

2.4. Plastome Sequence Divergence and Barcoding Investigation

Visualization of chloroplast genome sequence comparison results of 10 *Dendrobium* species using the online tool mVISTA, which showed the non-coding and coding regions of the 10 *Dendrobium* chloroplast genomes were almost the same (Figure 5), and the LSC (from *ndhJ* to $trnV^{UAC}$, *psbF* to *petL*) region and the SSC (from $trnN^{GUU}$ to *ndhA*) region were found to have the least similarity than the IR

Preprints (www.preprints.org) | NOT PEER-REVIEWED | Posted: 29 December 2023 doi:10.20944/preprints202312.2150.v1

regions. Given these results, there are many regions to develop DNA barcodes to differentiate *Dendrobium* species.

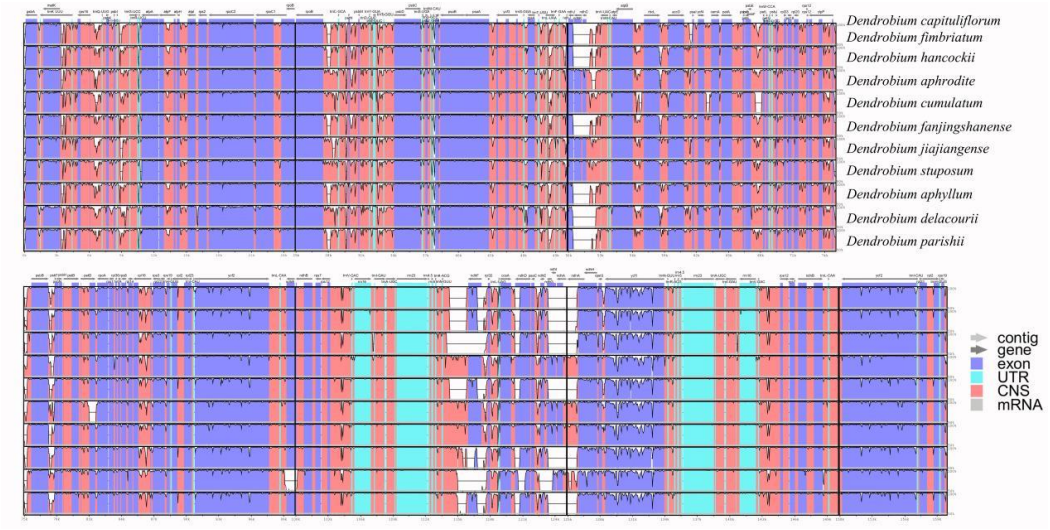

Figure 5. Global alignment of 10 *Dendrobium* plastomes using mVISTA with *D. capituliflorum* as reference. The *y*-axis shows the coordinates between the plastomes.

To further analyze mutational hotspots in *Dendrobium* plastids, we analyzed nucleotide diversity (Pi) using DnaSP6 for genome-wide comparisons (Figure 6, Supplementary Tables S3 and S4). The nucleotide diversity (Pi) values of the 10 plastomes ranged from 0 to 0.15089, We selected 5 mutational hotspots with Pi>0.10 (*rbcL-accD>atpB-rbcL>rbcL>trnL*^{UAA}*>accD*) as candidate barcodes. In protein-coding genes the results showed that at the cutoff point of Pi > 0.12, two coding sequences (*accD>ycf1*) had high nucleotide diversity and were suitable for phylogeny (Figure 6).

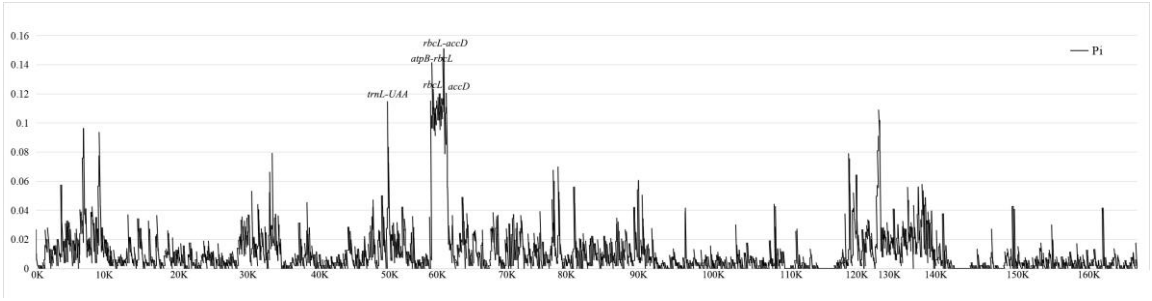

(**a**)

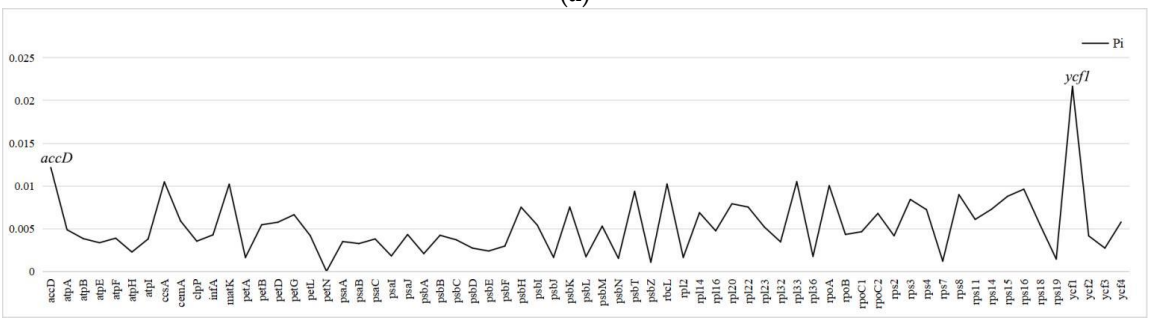

(**b**)

Figure 6. The length and informative site of *Dendrobium* plastome. (a)Protein-coding region; (b)IGS region.

2.5. IR Junctions' Contraction and Expansion

 doi:10.20944/preprints202312.2150.v1

The gene structure and positions of the IR junctions were well-conserved across the 10 *Dendrobium* species (Figure 7), with differences mainly in the length. At the adjacent regions of the LSC and IRb (JLB), the *rpl22* genes of the LSC crossed over into IRb. The junction between LSC and lRa (JLA), which were located in the *rps19* genes and *psbA* genes, except *D. fanjingshanense* and *D. Parishii* were located in the *rpl22* genes and *psbA* genes. The adjacent regions of SSC and lRb (JSB), which were located in the *ndhF* genes, except *D. aphrodite* and *D. delacourii* were lost the gene. While the *trnN* and *ycf1* genes were adjacent to the junction between SSC and IRa (JSA). The *ycf1* genes crossed 25 bp-1,082 bp over into IRa region, the degree of expansion varied greatly.

The main difference between the chloroplast genomes of different carbon assimilation pathways exists in the IR/SSC: in JSB regions, an overlap of *ycf1* and *ndhF* by 23-56 bp in *D. fimbriatum* (obligate C_3), *D. fanjingshanense* (facultative CAM), *D. aphyllum* and *D. Parishii* (constitutive CAM), which showing an increasing trend from C_3 to CAM; in JSA regions, an expansion of *ycf1* gene to IRa by 25 bp-1082 bp in the rest of species, which showing a decreasing trend from C_3 to CAM.

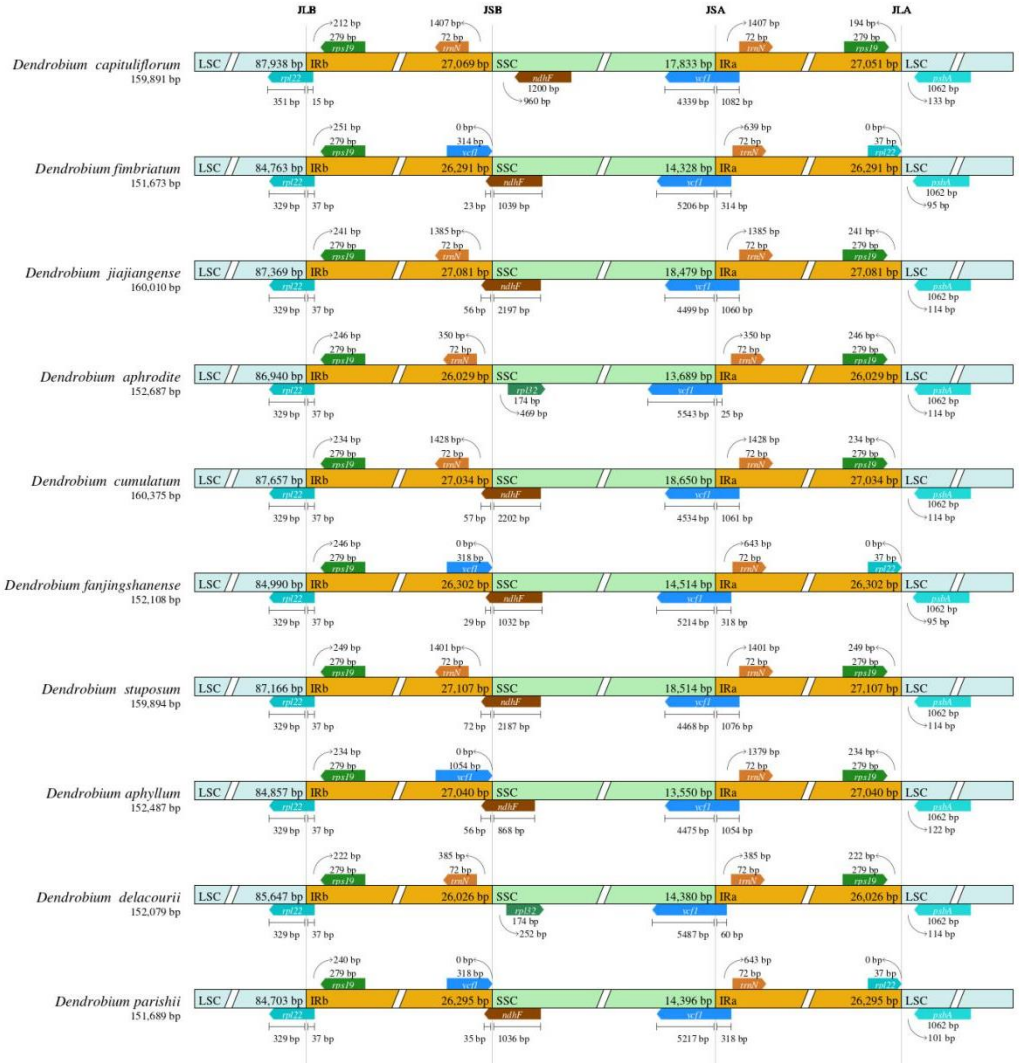

Figure 7. Comparison of the borders of the LSC, SSC and IR regions of 10 *Dendrobium* species.

2.6. Phylogenetic Analysis

The phylogenetic relationships inferred by ML, BI and MP analysis of the complete genomes predicted the same topology (Figure 8). In general, the phylogenetic trees revealed that the orchids have a monophyletic relationship with strong support (BS≥75%, PP≥0.90). Furthermore, the *Dendrobium* was monophyletic and was sister to *Bulbophyllum*. The constitutive CAM plants appeared independently at least twice in 10 *Dendrobium* species; the facultative CAM plants were discretedly

Preprints (www.preprints.org) | NOT PEER-REVIEWED | Posted: 29 December 2023 doi:10.20944/preprints202312.2150.v1

distributed. Character state reconstructions of *ndh* gene status across *Dendrobium* revealed a pattern of independent gene loss and pseudogenization (Figure 8). Character state optimization revealed that the complete *ndh* gene family was present in the ancestor of *Dendrobium*.

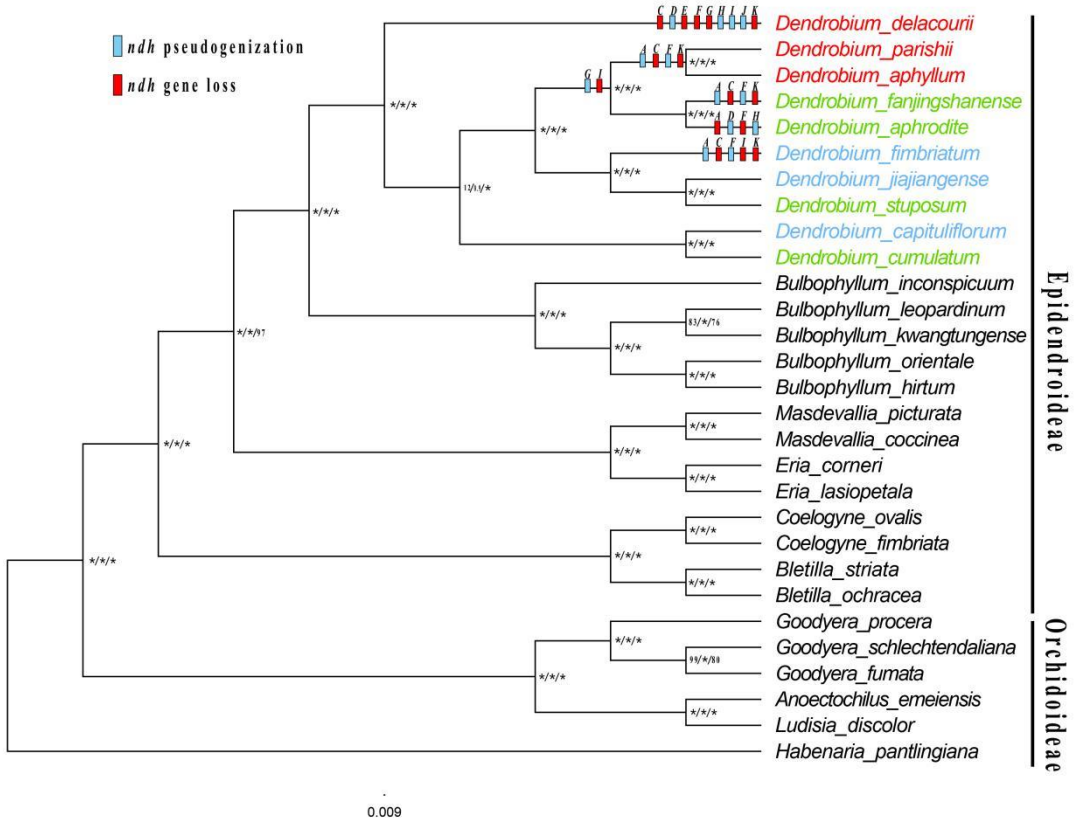

Figure 8. Phylogenetic tree of *Dendrobium* and the other 19 Orchid species based on the complete plastome data. Numbers near the nodes are bootstrap percentages and Bayesian posterior probabilities (BS_{ML} left, BS_{MP} middle and PP right). An asterisk (*) indicates that the node is 100 bootstrap percentage or 1.00 posterior probability. The constitutive CAM, obligate C_3 and facultative CAM species are shown in red, blue and green respectively. And Character reconstructions of *ndh* gene loss and pseudogenization events, mapped onto the phylogenetic tree.

3. Discussion

3.1. Identification the Photosynthetic Pathways Could Provide Vital Information for CAM Research

CAM is an important model of photosynthetic pathway, and plants with CAM pathway usually have higher water use efficiency and stronger drought tolerance [15,30]. *Dendrobium* is almost all epiphytic, with a wide distribution space and a large elevation range. The unique habitat and wide distribution of *Dendrobium* resulted in multiple photosynthetic pathways. However, because of the absence of a identification of photosynthetic pathways, the rich CAM resources of *Dendrobium* are still to be explored. Recently, whole-tissue carbon isotope ratios ($\delta^{13}C$) have been used to categorize species as C_3 or CAM predominantly [14]. However, $\delta^{13}C$ cannot identify species in which CAM was present in C_3 with the presence of stress. Therefore, we measured titratable acidity and net photosynthetic rates (Pn) to distinguish multiple photosynthetic pathways in *Dendrobium* more precisely. Based on the result, we confirmed that there were various photosynthetic pathways, including obligate C_3, facultative CAM and constitutive CAM among *Dendrobium* species. Based on the Pn in constitutive CAM plants were below zero during the day but enhanced that the night, which showed a very significant trend during nighttime, while in C_3 plants was expanded to zero during

 doi:10.20944/preprints202312.2150.v1

daytime but below night. Further combined with titratable acid values, constitutive CAM species had significant day-night titratable acid differences, C_3 plants which had non-significant day-night titratable acid differences were determined to be obligate C_3 plants, which showed significant differences were determined to be facultative CAM plants clearly. Combined with the comparative chloroplast genomic analysis, we believe we can provide new insights into the evolution of CAM.

3.2. The Plastome Characteristics

The size of the plastid genome of Orchidaceae has a large variation ranging from 19,047 bp (*Epipogium roseum*) [31] to 234,657 bp (*Cypripedium lichiangense*). The GC content ranged from 33.9% (*C. formosanum*) to 37.8% (*C. macranthos*) [32-34], and the number of genes was mostly around 130. Currently, the published plastids of *Dendrobium* members range from 148,431 bp (*D. zhenghuoense*) [35] to 160,123 bp (*D. thyrsiflorum*) [36]. In this study, we obtained the plastome sequences of 10 species of *Dendrobium* using next-generation sequencing technology. The plastome size ranges from 151,673 bp (*D. fimbriatum*) to 160,375 bp (*D. cumulatum*), the GC content ranged from 37.1% to 37.7% and the number of genes ranged from 127 to 132, located within the scope revealed by the reported orchid plastomes previously[31-32,37-40], but *D. cumulatum* will be the largest plastid genome in *Dendrobium*.

3.3. Plastome Structural Evolution Under Different Carbon Assimilation Pathways

In most angiosperms, plastid genomes are maternally inherited, thus maintaining a highly conserved structure in closely related species [41]. The contraction and expansion of IR region is a common phenomenon in the evolution process [42], which often affect the size of the entire chloroplast genome and is the main driving force for the structural variation of chloroplast genome [43-45]. The difference of IR/SC boundary is more significant in Orchids [46,47], so Luo et al. [34] divided chloroplast genomes of orchids into four categoriesand and two evolutionary routes by the differences: (1) the *ycf1* gene within the SSC region expands toward IRa, causing *ycf1* in the IRb region to move toward the border and overlap with the *ndhF* gene; (2) the *ycf1* gene within the SSC region continues to move toward the interior of the SSC region, and the portion of the coding region that is located at the border becomes shorter and shorter, after which the *ycf1* gene is completely embedded in the SSC region. In this study, we observed some difference in the IR/SC boundary regions of different carbon assimilation pathways in *Dendrobium* plastomes. First, in JSB regions, an overlap of *ycf1* and *ndhF* by 23-56 bp, which showing an increasing trend from C_3 to CAM; second, in JSA regions, an expansion of *ycf1* gene to IRa by 25 bp-1082 bp, which showing a decreasing trend from C_3 to CAM, which correspond to the two evolutionary routes of Luo, respectively, these findings suggest that the evolution of the IR/SC boundary is different between different carbon assimilation pathways.

The plastid genome size of structural CAM plants was 151,689 bp to 152,487 bp, which were shorter than that of obligate C_3 plants (151,673 bp-160,010 bp) and facultative CAM plants (152,108 bp-160,375 bp). The main difference is the phenomenon that *ndh* gene loss or pseudogenization in constitutive CAM plants. This phenomenon was observed in 6 of 10 *Dendrobium* species, including 3 constitutive CAM plants (100%), 2 facultative CAM plants (50%), and 1 obligate C_3 plant (33%). Although the *ndh* genes have been detected in the mitochondrial (mt) genomes of some orchids, there is no direct evidence whether these genes are related to the loss of *ndh* genes in plastids [33]. Therefore, the mechanism of *ndh* gene loss and pseudoplasmaization in orchids needs to be further investigated. In addition, studies have suggested that the loss of *ndh* genes in *Littorella* (Plantaginaceae) can possibly related to their amphibious lifestyle and partial dependence on CAM photosynthesis [48]. Liu et al. [32] studied the Aeridinae were all constitutive CAM plants and all of them were *ndh* loss or pseudogenization, what's more, the constitutive CAM plants in our study also *ndh* gene loss or pseudogenization, and this phenomenon accounted for a decreasing proportion of constitutive CAM, facultative CAM, and obligate C_3 plants, it is speculated that the loss of the *ndh* gene may be closely related to the CAM pathway.

 doi:10.20944/preprints202312.2150.v1

3.4. The Barcoding Investigation and Phylogenetic Analysis

Nucleotide diversity (Pi) is an important indicator that can be used to assess genetic differences between different species, and the position with higher variability in the nucleic acid sequences can be used to infer evolutionary relationships [49,50]. In addition, the genetic loci used for DNA barcoding usually contain enough informative loci to effectively define closely related species[51], which has been used to identify *Dendrobium* species[52-54]. In this study, the nucleotide diversity analysis on intact plastids of *Dendrobium*, five highly variable regions were identified and protein-coding genes identified two highly variable coding genes. The seven highly variable regions identified in this study can be used as DNA molecular markers to distinguish *Dendrobium* relatives, and the results can be used to develop *Dendrobium* DNA barcodes.

Repeated sequences have the advantages of rich polymorphism, high repeatability and good co-dominance [55], which play an important role in species evolution as well as identification of relatives [56,57], often used in the study of genetic diversity and systematic relationships of taxa[58-61].In orchids, SSR markers have been widely used in *Cymbidium* [62], *Yucca* [63], *Phalaenopsis* [64,65] and *Dendrobium* [66,67], which mononucleotides and dinucleotides are prevalent and highly abundant [68,69]. In this study, a total of 41–60 SSRs were identified from *Dendrobium* plasmids, indicating that the plasmid genome of *Dendrobium* retained abundant genetic information. Most of the SSRs are mononucleotide and dinucleotides repeat in these 10 *Dendrobium* species, in the range of 68% to 90%; similar results are found in most orchids [70-73]. Compared with *D. nobile*, which has a trinucleotide content of up to 37% [74], the average trinucleotide content in our study was only about 4%, and even *D. delacourii* did not has trinucleotides (Supplementary TableS5), which is probably due to a more conserved SSR [75]. The above findings can provide a data basis for further studies on population genetics.

Our results revealed the multiple independent CAM origins exist in *Dendrobium* species. Despite being a valuable class of plants in water conservation and drought resistance, there are few studies on the evolution in CAM plants. Orchidaceae family is the most distributed group of CAM pathways, recent studies have shown that the constitutive CAM pathway has evolved at least nine times in *Bulbophyllum* [76,77], and have evolved independently at least eight times in *Dendrobium* [14]. The identification of facultative CAM plants is relatively difficult, so there is little literature on the evolution of facultative CAM pathways. In our study, the significance of diurnal titrable acid and net photosynthetic rates curve were measured, four facultative CAM plants and three constitutive CAM plants were identified. The results supported that the three constitutive CAM plants originated independently twice in the plastid phylogenetic genomics tree, and facultative CAM plants showed discrete distribution with high support for each branch. And Our results strongly imply that the ancestral *Dendrobium* plastome possessed full ORFs for all *ndh* genes.

4. Materials and Methods

4.1. Plant Materials

The materials used in this study are the species with complete chloroplast genome data in NCBI (https://www.ncbi.nlm.nih.gov/) and some ex-situ protected native species. Ten *Dendrobium* species were selected, including *D. aphrodite, D. capituliflorum, D. cumulatum, D. delacourii, D. jiajiangense, D. stuposum, D. aphyllum, D. fanjingshanense, D. fimbriatum and D. parishii*. They were cultivated in the Fujian Agriculture and Forestry University, Fujian province, China. Their voucher information is given in Supplementary Table S1.

4.2. Determination of Photosynthetic Pathways

4.2.1. Determination of Whole-tissue Carbon Isotope Ratios

Healthy leaves of each species were sampled about 2g, dried and preserved with silica gel. The dried leaves were put into a 10mL centrifugal tube, crushed with a ball mill (JXFSTPRP-64), and weighed with 4mg for package sample. At the Ecological Stable Isotope Center, College of Forestry,

 doi:10.20944/preprints202312.2150.v1

Fujian Agriculture and Forestry University, Stable isotope Mass Spectrometer (IsoPrime100, Limonta, Germany) was used to analyze the samples, and standard samples (acetanilide, L-histidine, D-glutamic acid and glycine) were used for data calibration. The carbon isotope value ($\delta^{13}C$) of the sample was calculated by the formula:

$$\delta^{13}C(‰)=[(sample^{13}C/^{12}C)/(standard^{13}C/^{12}C)^{-1}]\times1000 \quad (1)$$

The accuracy of the measured value is less than 0.2‰.

4.2.2. Determination of Titratable Acidity

The diurnal fluctuation of total organic acid content per unit fresh weight of leaves is one of the indicators reflecting the photosynthetic pathway. Under clear weather conditions, soil hygrometer L99-TWS-1 was used to measure the matrix free water content of potting soil. Plants under drought stress (five days after matrix humidity dropped to 0) were selected as test objects, and the third to fifth mature healthy leaves were sampled. The sampling time was day (between 5:00 and 6:20) and night (between 17:45 and 16:30). Three repeat samples were taken at each time period. After all samples were collected, they were cleaned and disinfected with alcohol, wiped dry, and immediately stored in liquid nitrogen. Total organic acids were determined by indicator titration [78]. The specific preparation and operation methods are as follows:

1. Reagent

Reagent I: 1% phenolphthalein solution, 1g phenolphthalein dissolved in 60ml anhydrous ethanol and 40ml water;

Reagent II: c(NaOH)=0.01mol L^{-1}, 0.04 gNaOH dissolved in 100ml water.

2. Equipment

10ml beaker, Centrifuge, Grinding machine, Manual single channel pipette (10μl~100μl adjustable).

3. Titration steps

Add 1g sample to 10ml water, grind it into homogenate in a grinder, centrifuge at 8000rpm at 4°C for 10min, add 0.5ml supernatant to 9.5ml water in a small beacher, add 10μl reagent I, titrate with reagent II until the light red color does not disappear, record the volume of NaOH used. The total titrated acid is calculated, and the acid content is expressed as the molar amount of OH^- consumed per unit of fresh weight tissue. The formula is as follows:

$$N=(V/1000)\times C/(W/1000) \quad (2)$$

N: the consumption of OH^- per kilogram of fresh weight tissue (mol kg^{-1} FW);

V: the volume of NaOH solution consumed at the end of the titration (ml);

C: the concentration of NaOH solution (mol L^{-1});

W: the mass of the sample (g).

Refer to previous studies [76,79]. The mean value and standard deviation of the three repeated values were calculated respectively, and then the difference of the day and night mean value and standard deviation was made in pairs respectively to determine whether there was a significant difference by comparing the size of the two differences: difference of the mean value>sum of the standard deviation, there is a significant difference; on the contrary, there is no significant difference.

4.2.3. Determination of the Net Photosynthetic Rate

The whole experiment process was completed in the artificial climate chamber with controlled conditions: the temperature was 28°C during the day (6:00-18:00, 200 μmol $m^{-2}s^{-1}$ light treatment) and 22°C at night (18:00-6:00, dark treatment) [80], with an air relative humidity of 40%. The detailed steps are as follows: the volumetric water content of the matrix was determined using the soil hygrometer L99-TWS-1, and the experiment was conducted five days after the drop to 0. The third to fifth mature

 doi:10.20944/preprints202312.2150.v1

healthy leaves were selected and the CO_2 exchange rate was measured for 24h by using the portable photosynthetic apparatus Li-6400XT, transparent bottom leaf chamber and 6400-02B red and blue light source. The measuring system is equipped with a 10L air buffer bottle, the gas flow rate is 500μms, the value interval is 5min, and the whole-day photosynthesis curve is drawn. Perform a match correction before each value.

4.3. DNA Extraction and Sequencing

In this study, Six of ten *Dendrobium* species were newly sequenced. 2g fresh plant leaves were sampled and snap-frozen in liquid nitrogen and stored in an ultra-low temperature refrigerator at -80°C. The total DNA was isolated using a modified CTAB method [81]. The total DNA of the samples was extracted by Dneasy Plant Mini Kits (QIAGEN, Germany), and then detected by agarose gel electrophoresis, and the DNA with more than 1μg of extracted amount and obvious main bands was selected. The total DNA from the samples was randomly interrupted to construct a 150 bp Denovo small fragment libraries, which was sequenced by the Beijing Genomics Institute (Shenzhen, China) on the Illumina HiSeq 2500 platform, and 20 Gb of raw data were obtained from each sample, which were filtered to obtain at least 10 Gb the final high-quality data (clean data) for subsequent data analysis.

4.4. Plastome Assembly and Annotation

Plasmid assembly and annotation were performed according to previous methods [82]. The paired-end reads were assembled using the GetOrganelle pipeline (https://github.com/Kinggerm/GetOrganelle), and then, the filtered reads were assembled using SPAdes version 3.10 [83]. Assembled the chloroplast genome using the published plastome of *D. thyrsiflorum*(MN306203) as the reference sequence. The gene annotation using DOGMA [84] based on default parameters and calibrated with Geneious Prime v2021.1.1 [85]. Genome-wide mapping of chloroplasts using OGDRAW [86].

4.5. Genome Comparison and Analysis, IR Border and Divergence Analyses

Repeat sequence analysis, diversity analysis and IR boundary analysis

The plastome genomes across the ten species of *Dendrobium* were visualized with mVISTA using the LAGAN alignment program [87] with the sequence of *D. capituliflorum* as a reference. The rearrangements of plastomes were detected and plotted using Mauve of ten species [88]. Contraction and expansion of IR boundaries in the chloroplast genomes of 10 *Dendrobium* plants were measured and compared using the online program IRscope (https://irscope.shinyapps.io/irapp/) [89]. Mutation hotspot regions and genes were aligned to the plastid sequences using MAFFT v7 [90]. The nucleotide diversity (Pi) of the 10 plastids of *Dendrobium* was then calculated using DnaSP v6.12.03 (DNA sequence polymorphism) [91]. Highly mutated hotspot regions were identified by a sliding window strategy. The step size was set to 25 bp and the window length was 100 bp.

4.6. Repeat Sequence Analysis

Simple Sequence Repeats (SSRs) of 10 *Dendrobium* species were identified and localized using MISA-web, where the number of mononucleotide, dinucleotide, trinucleotide, tetranucleotide, pentanucleotide and hexanucleotide repeats were set to 10, 5, 4, 3, 3, 3, 3, and 3 respectively [92]. The online REPuter software (https://bibiserv.cebitec.uni-bielefeld.de/reputer) was used to identify interspersed nuclear elements (INE), including forward, reverse, palindrome, and complement sequences, setting the maximum number of repetitive sequences to 50 and the minimum repetition size to 8, the hamming distance was set to 3 [93].

4.7. Phylogenetic Reconstruction

Phylogenetic analysis of 29 species of Orchidaceae using complete plastid genomes. Of these 29 species, 6 *Dendrobium* species are our newly sequenced and the complete plasmid data of other 23 species were publicly available from NCBI. A list of taxa analyzed with voucher information and GenBank accessions is shown in Supplemental Table S1. The whole plastome fasta sequences of the genus *Dendrobium* and its outgroups were aligned using Geneious Prime v2021.1.1 [85], then used the CIPRES Science Gateway to construct phylogenetic trees for the maximum likelihood (ML), Maximum Parsimony (MP) and Bayesian Inference (BI) phylogenetic trees[94]. The ML tree was constructed using the GTRGAT nucleotide substitution model using the Bootstrap algorithm with 1000 repetitions and the rest of the parameters as default [95]. The MP tree was constructed using a heuristic search and branch exchange algorithm (TBR), where all nucleotide traits were equally weighted and searched with an arbitrary repetition of 1,000 times, and the reliability of the phylogenetic tree was analyzed with a 1,000 repetitions of a self-expansion method (Bootstrap) [96].The BI tree was constructed using the GTR+I+Γ model with the Markov Chain Monte Carlo (MCMC) method, where each of the four Markov chains was run for 10,000,000 generations, with samples taken every 100 generations, and the top 25% of the trees were discarded as burn-in samples to ensure that each chain reached a stable state (Ronquist et al., 2012). The first 25% of the trees are discarded as burn-in samples to ensure that each chain reaches a steady state, and finally the posterior probability (PP) of each branch is obtained [97].

5. Conclusions

Our research based on the results of $\delta^{13}C$, net photosynthetic rates (Pn) and titratable acid value, identified 10 *Dendrobium* species into three photosynthetic pathways. Then the chloroplast whole genome characteristics of them were analyzed which shows that the overall structure and gene content of the plastomes of 10 *Dendrobium* species are relatively conserved, with only certain differences in genome size, gene content, GC content, repeat sequences. Among multiple photosynthetic pathways, the chloroplast genome size of constitutive CAM plants is shorter because of their *ndh* gene loss or pseudogenization, the loss of the *ndh* gene may be closely related to the CAM pathway. What's more, the evolution of the IR/SC boundary is different between different carbon assimilation pathways. Phylogenetic analyses showed that there are multiple independent CAM origins in selected *Dendrobium* species, and the ancestral *Dendrobium* plastome possessed full ORFs for all *ndh* genes. The study aims to clarify the chloroplast genomic features of different photosynthetic pathways, enrich the genomic data of CAM plants in *Dendrobium*.

Supplementary Materials: The following supporting information can be downloaded at the website of this paper posted on Preprints.org.

Author Contributions: Conceptualization, methodology, Y.L., Z.L. and M.L.; Software, formal analysis, visualization, Y.L.; Investigation, resources and data curation, Y.L., S.Z. and J.D.; writing—original draft preparation, Y.L.; writing—review and editing, J.S., D.L., S.L., Z.L. and M.L.; supervision, Y.L. Z.L. and M.L.; project administration, M.L.; funding acquisition M.L. All authors have read and agreed to the published version of the manuscript.

Funding: This research was supported by the National Key Research and Development Program **o**f China (2023YFD1600504).

Institutional Review Board Statement: Not applicable.

Informed Consent Statement: Not applicable.

Data Availability Statement: All the data are provided within this manuscript and supplementary materials.

Acknowledgments: We acknowledge the technical support of laboratory staff during the conduction of laboratory experiments, Ding-Kun Liu, Xiong-De Tu, and Cheng-Yuan Zhou.

Conflicts of Interest: The authors declare no conflict of interest.

References

1. Rodrigues, M. A.; Matiz, A.; Cruz, A. B.; Matsumura, A. T.; Takahashi, C. A.; Hamachi, L.; Fe´lix, L. M.; Pereira, P. N.; LatansioAidar, S. R.; Aidar, M. P. M.; Demarco, D.; Freschi, L.; Mercier, H.; Kerbauy, G. B. Spatial pattems of photosynthesis in thin and thickleaved epiphytic orchids: Unravelling C_3-CAM plasticity in an organ-compartmented way. *Annals of Botany* **2013**, 1 12(1): 17_29.
2. Winter, K.; Holtum, J. A. M.; Smith, J. A. C. Crassulacean acid metabolism: a continuous or discrete trait? *New Phytologist* **2015**, 208(1): 73–78.
3. Niechayev, N. A.; Pereira, P. N.; Cushman, J. C. Understanding trait diversity associated with crassulacean acid metabolism (CAM). *Current Opinion in Plant Biology* **2019**, 49: 74–85.
4. Wickell, D.; Kuo, L. Y.; Yang, H. P.; Ashok, A. D.; Irisarri, I.; Dadras, A.; de Vries, S.; de Vries, J.; Huang, Y. M.; Li, Z.; Barker, M. S.; Hartwick, N. T.; Michael, T. P.; Li, F. W. Underwater CAM photosynthesis elucidated by *Isoetes* genome. *Nature Communications* **2021,** 12: 6348.
5. Silvera, K. M.; Neubig, M.; Whitten, W. M.; Williams, N. H.; Winter, K.; Cushman, J. C. Evolution along the crassulacean acid metabolism continuum. *Functional Plant Biology* **2010**, 37 (11): 995–1010.
6. Cai, J.; Liu, X.; Vanneste, K.; Proost, S.; Tsai, W. C.; Liu, K. W.; Chen, L. J.; He, Y.; Xu, Q.; Bian, C.; Zheng, Z.; Sun, F.; Liu, W.; Hsiao, Y. Y.; Pan, Z. J.; Hsu, C. C.; Yang, Y. P.; Hsu, Y. C.; Chuang, Y. C.; Dievart, A.; Dufayard, J. F.; Xu, X.; Wang, J. Y.; Wang, J.; Xiao, X. J.; Zhao, X. M.; Du, R.; Zhang, G. Q.; Wang, M.; Su, Y. Y.; Xie, G. C.; Liu, G. H.; Li, L. Q.; Huang, L. Q.; Luo, Y. B.; Chen, H. H.; Van de Peer, Y.; Liu, Z. J. The genome sequence of the orchid *Phalaenopsis equestris*. *Nat Genet* **2015**;47(1):65–72.
7. Yang, X. H.; Cushman, J. C.; Borland, A. M.; Edwards, E. J.; Wullschleger, S. D.; Tuskan, G. A.; Owen, N. A.; Griffiths, H.; Smith, J. A. C.; De, P. L.; Henrique, C.; Weston, D. J.; Cottingham, R.; Hartwell, J.; Davis, S. C.; Silvera, K.; Ming, R.; Schlauch, K.; Abraham, P.; Stewart, J. R.; Guo, H. B.; Albion, R.; Ha, J. M.; Lim, S. D.; Wone, B. W. M.; Yim, W. C.; Garcia, T.; Mayer, J. A.; Petereit, J.; Nair, S. S.; Casey, E.; Hettich, R. L.; Ceusters, J.; Ranjan, P.; Palla, K. J.; Yin, H.; Reyes-García, C.; Andrade, J. L.; Freschi, L.; Beltrán, J. D.; Dever, L. V.; Boxall, S. F.; Waller, J.; Davies, J.; Bupphada, P.; Kadu, N.; Winter, K.; Sage, R. F.; Aguilar, C. N.; Schmutz, J.; Jenkins, J.; Holtum, J. A. M. A roadmap for research on crassulacean acid metabolism (CAM) to enhance sustainable food and bioenergy production in a hotter, drier world. *New Phytologist* **2015**, 207(3): 491–504.
8. Valdez-Hernández, M.; González-Salvatierra, C.; Reyes-García, C.; Jackson, P. C.; Andrade, J. L. Physiological Ecology of Vascular Plants. In: Islebe GA, et al.,editors. Biodiversity and Conservation of the Yucatán Peninsula. International Publishing Switzerland: Springer; **2015.** p. 97–129.
9. Hermida-Carrera, C.; Fares, M. A.; Font-Carrascosa, M.; Kapralov, M. V.; Koch, M. A.; Mir, A; Molins, A; Ribas-Carbó, M; Rocha, J.; Galmés, J. Exploring molecular evolution of Rubisco in C_3 and CAM Orchidaceae and Bromeliaceae. *BMC Evol Biol* **2020**; 20(1): 11.
10. Silvera, K.; Santiago, L. S.; Cushman, J. C.; Winter,K. The incidence of crassulacean acid metabolism in Orchidaceae derived from carbon isotope ratios: a checklist of the flora of Panama and Costa Rica. *Botanical Journal of the Linnean Society* **2010**, 163(2): 194–222.
11. Christenhusz, M. J. M.; Byng, J. W. The number of known plants species in the world and its annual increase. *Phytotaxa* **2016**, 261: 201–217.
12. Winter, K.; Wallace, B. J.; Stocker, G. C.; Roksandic, Z. Crassulacean acid metabolism in Australian vascular epiphytes and some related species. *Oecologia* **1983**, 57(1–2): 129–141.
13. Silvera, K.; Santiago, L. S.; Cushman, J. C.; Winter, K. Crassulacean acid metabolism and epiphytism linked to adaptive radiations in the Orchidaceae. *Plant Physiology* **2009**, 149 (4): 1838–1847.
14. Li, M. H.; Liu, D. K.; Zhang, G. Q.; Deng, H.; Tu, X. D.; Wang, Y.; Lan, S. R.; Liu, Z. J. A perspective on crassulacean acid metabolism photosynthesis evolution of orchids on different continents: *Dendrobium* as a case study. *Journal of Experimental Botany* **2019** 70 (22): 6611–6619.
15. Schweiger, A. H.; Nürk, N. M.; Beckett, H.; Liede-Schumann, S.; Midgley, G. F.; Higgins, S. I. The eco-evolutionary significance of rainfall constancy for facultative CAM photosynthesis. *New Phytologist* **2021**, 230: 1653–1664.
16. Winter. K. Ecophysiology of constitutive and facultative CAM photosynthesis *J. Exp. Bot.*, **2019,** 70(22): 6495-6508.
17. Su, W. H.; Zhang, G. F. Primary Study on Photosynthetic Characteristics of *Dendrobium nobile*. *Traditional Chinese medicinal materials* **2003**, 26: 157–159.
18. Su, W. H.; Zhang, G. F. The photosynthesis pathway in leaves of *Dendrobium officinale*. *Acta Phytoecologica Sinica* **2003,** 27: 631–637.
19. Ren, J. W.; Wang. Y.; Pen, Z. H.; Hu, Q. Measurement of Malic Acid Diel Fluctuation of Leaves in Three Dendrobia. *Acta Agriculturae Universitis Jiangxiensis* **2010**, 32(3): 547–552.
20. Liu, Z. D. The study of transformation mechanism of morphology and physiology in the switch from C_3-photosynthesis to Crassulacean acid metabolism of *Dendrobium*. *HuaZhong Agricultural University* **2014**.
21. Qiu, S.; Sultana, S.; Liu, Z. D.; Yin, L. Y.; Wang, C. Y. Identification of obligate C_3 photosynthesis in *Dendrobium*. *Photosynthetica: International Journal for Photosynthesis Research* **2015,** (53-2).

22. Zou, L. H.; Wan, X.; Deng, H.; Zheng, B. Q.; Yan, B. J. RNA-seq transcriptomic profiling of crassulacean acid metabolism pathway in *Dendrobium catenatum*. *Scientific Data* **2018**, 5(1): 180252.
23. Zou, L. H. Crassulacean Acid Metabolism Pathway and Its Key Genes' Co-expression Networks in *Dendrobium catenatum*. BeiJing: *Chinese Academy of Forestry* **2019.**
24. Zeng, M. Y.; Xu, S. W.; Wang, F. J.; Lin,Y, J.; Zhang, S.;Lan, S. R.; Li, M. H. Measurement of Carbon Assimilation Pathway for the Mainly Native Species of Parents in Nobile Type *Dendrobium*. *Molecular Plant Breeding* **2023,** https://link.cnki.net/urlid/46.1068.S.20230912.1030.002.
25. Xue, Q. Q.; Yang, J. P.; Yu, W. H.; Wang, H. M.; Hou, Z. Y.; Li, C.; Xue, Q. Y.; Liu, W.; Ding, X. Y.; Niu, Z. T. The climate changes promoted the chloroplast genomic evolution of *Dendrobium* orchids among multiple photosynthetic pathways. *BMC Plant Biology* **2023,** Vol.23(No.1)：189.
26. Liu, H. Y.; Liu, L. K.; Wang, Z. L.; Yu L. M.; Li J. P.; Zeng Y. Research Progress on Chloroplast Genome of Orchidaceae. *Chinese Wild Plant Resources* **2023**, Vol. 42 No. 7 Jul: 73-79.
27. Niu, Z; Xue, Q; Zhu, S; Jing, S; Liu, W; Ding, X. The complete plastome sequences of four orchid species: insights into the evolution of the Orchidaceae and the utility of plastomic mutational hotspots. *Front Plant Sci* **2017,** 8: 715.
28. Zhu, S; Niu, Z; Xue, Q; Hui, W.; Xie, X.; Ding, X. Accurate authentication of *Dendrobium officinale* and its closely related species by comparative analysis of complete plastomes. *Acta Pharmaceutica Sinica B* **2018**, 8(06): 969-980.
29. Osmond, C. B.; Allaway, W. G.; Sutton, B. G.; Troughton, J. H.; Winter, K. Carbon isotope discrimination in photosynthesis of CAM plants. *Nature* **1973,** 246(5427): 41–42.
30. Borland, A. M.; Griffiths, H.; Hartwell, J.; Smith, J. A. Exploiting the potential of plants with crassulacean acid metabolism for bioenergy production on marginal lands. *Journal of Experimental Botany* **2009,** 60(10): 2879–2896.
31. Schelkunov, M. I.; Shtratnikova, V. Y.; Nuraliev, M. S.; Selosse, M. A.; Penin, A. A.; Logacheva, M. D. Exploring the limits for reduction of plastid genomes: A case study of the mycoheterotrophic orchids *Epipogium aphyllum* and *Epipogium roseum*. *Genome Biol. Evol* **2015,** 7, 1179–1191.
32. Liu, D. K.; Tu, X. D.; Zhao, Z.; Zeng, M. Y.; Zhang, S.; Ma, L.; Zhang, G. Q.; Wang, M. M.; Liu, Z. J.; Lan, S. R.; Li, M. H.; Chen, S. P. Plastid phylogenomic data yield new and robust insights into the phylogeny of Cleisostoma–Gastrochilus clades (Orchidaceae, Aeridinae). *Molecular Phylogenetics and Evolution* **2020,** 145:106729.
33. Lin, C. S.; Chen, J. J.; Huang, Y. T.; Chan, M. T.; Daniel, H.; Chang, W. J.; Hsu, C. T.; Liao, D. C.; Wu, F. H.; Lin, S. Y.; Liao, C. F.; Deyholos, M. K.; Wong, G. K.; Albert, V. A.; Chou, M. L.; Chen, C. Y.; Shih, M. C. The location and translocation of *ndh* genes of chloroplast origin in the Orchidaceae family. *Sci Rep* **2015,** 5: 9040.
34. Luo, J.; Hou, B. W.; Niu, Z. T.; Liu, W.; Xue, Q. Y.; Ding, X. Y. Comparative chloroplast genomes of photosynthetic orchids: insights into evolution of the Orchidaceae and development of molecular markers for phylogenetic applications. *PloS One* **2014,** 9 (6): e99016.
35. Huang, Y. Z.; Zhuang, L. B.; Zhai, J. W.; Lin, W. J. The complete chloroplast genome sequence of *Dendrobium zhenghuoense* (Orchidaceae). *Mitochondrial DNA Part B* **2019,** Vol.4(No.2): 3326-3327.
36. Pan, Y. Y.; Li, T. Z.; Chen, J. B.; Huang, J.; Rao, W. H. Complete chloroplast genome of *Dendrobium thyrsiflorum* (Orchidaceae)(Article). *Mitochondrial DNA Part B: Resources* **2019,** Vol.4(No.2): 3192-3193.
37. Guo, Y. Y; Yang, J. X.; Li, H. K.; Zhao, H. S. Chloroplast genomes of two species of *Cypripedium*: Expanded genome size and proliferation of AT-biased repeat sequences. *Frontiers in Plant Science* **2021,** 12: 609729.
38. Kim, Y. K.; Jo, S.; Cheon, S. H.; Joo, M. J.; Hong, J. R.; Kwak, M.; Kim, K. J. Plastome Evolution and Phylogeny of Orchidaceae, with 24 New Sequences. *Front. Plant Sci* **2020,** 11, 22.
39. Ye, B. J.; Zhang, S.; Tu, X. D.; Liu, D. K.; Li, M. H. The complete plastid genome of *Thrixspermum tsii* (Orchidaceae, Aeridinae). *Mitochondrial DNA Part B* **2020,** 5, 384–385.
40. Guo, Y. Y.; Yang, J. X.; Bai, M. Z.; Zhang, G. Q.; Liu, Z. J. The chloroplast genome evolution of Venus slipper (*Paphiopedilum*): IR expansion, SSC contraction, and highly rearranged SSC regions. *BMC Plant Biol* **2021,** 21, 248.
41. Wicke, S.; Schneeweiss, G. M.; DePamphilis, C. W.; Müller, K. F.; Quandt, D. The evolution of the plastid chromosome in land plants: Gene content, gene order, gene function. *Plant Mol. Biol* **2011,** 76, 273–297.
42. Huang, H.; Shi, C.; Liu, Y.; Mao, S. Y.; Gao, L. Z. Thirteen *Camellia* chloroplast genome sequences determined by high-throughput sequencing: Genome structure and phylogenetic relationships. *BMC Evol. Biol* **2014,** 14, 151.
43. Kim, K. J. Complete chloroplast genome sequences from Korean ginseng (Panax schinseng Nees) and comparative analysis of sequence evolution among 17 vascular plants. *DNA Research* **2004,** 11(4): 247-261.
44. Raubeson, L. A.; Peery, R.; Chumley, T. W.; Dziubek, C.; Fourcade, H. M.; Boore, J. L.; Jansen, R. K. Comparative chloroplast genomics: Analyses including new sequences from the angiosperms Nuphar advena and *Ranunculus macranthus*. *BMC Genom* **2007**, 8, 174.

45. Dugas, D. V.; Hernandez, D.; Koenen, E. J.; Schwarz, E.; Straub, S.; Hughes, C. E.; Jansen, R. K.; Nageswara-Rao, M.; Staats, M. Mimosoid legume plastome evolution: IR expansion, tandem repeat expansions, and accelerated rate of evolution in clpP. *Sci. Rep* **2015**, 5, 16958.
46. Wang, W. C.; Chen, S. Y.; Zhang, X. Z. Whole-genome comparison reveals divergent IR Borders and mutation hotspots in chloroplast genomes of herbaceous bamboos (Bambusoideae: Olyreae). *Molecules* **2018,** 23(7):1537.
47. Park, S.; An, B.; Park, S. Reconfiguration of the plastid genome in *Lamprocapnos spectabilis*: IR boundary shifting, inversion, and intraspecific variation. *Scientific Reports* **2018,** 8(1): 1-14.
48. Mower, J. P.; Guo, W. H.; Partha, R.; Fan, W.; Levsen, N.; Wolff, K.; Nugent, J. M.; González, N. Plastomes from tribe Plantagineae (Plantaginaceae) reveal infrageneric structural synapormorphies and localized hypermutation for *Plantago* and functional loss of *ndh* genes from *Littorella. Molecular phylogenetics and evolution* **2021,** 107217.
49. Ding, S.; Dong, X.; Yang, J.; Guo, C.; Cao, B.; Guo, Y.; Hu, G. Complete Chloroplast Genome of *Clethra fargesii* Franch., an Original Sympetalous Plant from Central China: Comparative Analysis, Adaptive Evolution, and Phylogenetic Relationships. *Forests* **2021,** 12, 441.
50. Abdullah; Mehmood, F.; Shahzadi, I.; Waseem, S.; Mirza, B.; Ahmed, I.; Waheed, M. T. Chloroplast genome of *Hibiscus rosasinensis* (Malvaceae): Comparative analyses and identification of mutational hotspots. *Genomics* **2020,** 112, 581–591.
51. Chen, J. L.; Wang, F.; Zhou, C. Y.; Ahmad, S.; Zhou, Y. Z.; Li, M. H.; Liu, Z. J.; Peng, D. H. Comparative Phylogenetic Analysis for *Aerides* (Aeridinae, Orchidaceae) Based on Six Complete Plastid Genomes. *International journal of molecular sciences* 2023, Vol.24(No.15): 12473.
52. Xu, S. Z.; Li, D, Z.; Li, J. W.; Xiang, X. G.; Jin, W. T.; Huang, W. C.; Jin, X. H.; Huang, L. Q. Evaluation of the DNA barcodes in *Dendrobium* (Orchidaceae) from mainland Asia. *PLoS ONE* **2015,** 10, e0115168.
53. Niu, Z. T.; Zhu, S. Y.; Pan, J. J.; Li, L. D.; Sun, J.; Ding, X. Y. Comparative analysis of *Dendrobium* plastomes and utility of plastomic mutational hotspots. *Sci. Rep* **2017**, 7, 2073.
54. Feng, S. G.; Jiang, Y.; Wang, S.; Jiang, M. Y.; Chen, Z.; Ying, Q. C.; Wang, H. Z. Molecular identification of *Dendrobium* species (Orchidaceae) based on the DNA barcode ITS2 region and its application for phylogenetic study. *International Journal of Molecular Sciences* **2014,** 16, 21975–21988.
55. Sun, Z. X.; Ao, P. X.; Bi, Y. F.; Zhao, Y. Complete Chloroplast Genome Sequence and Characteristics Analysis of *Medicago sativa*'Deqin'. *Acta Agrestia Sinica* **2022**, 30(02):320-328.
56. Chen, Y.; Hu, N.; Wu, H. Analyzing and characterizing the chloroplast genome of *Salix wilsonii. BioMed Res. Int* **2019,** 5190425.
57. Khan, A.; Asaf, S.; Khan, A. L.; Al-Harrasi, A.; Al-Sudairy, O.; AbdulKareem, N. M.; Khan, A.; Shehzad, T.; Alsaady, N.; Al-Lawati, A.; Al-Rawahi, A; Shinwari, Z. K. First complete chloroplast genomics and comparative phylogenetic analysis of *Commiphora gileadensis* and *C. foliacea*: Myrrh producing trees. *PLoS One* **2019**, 14, e0208511.
58. Yu, J.; Dossa, K.; Wang, L.; Zhang, Y.; Wei, X.; Liao, B.; Zhang, X. PMDBase: A database for studying microsatellite DNA and marker development in plants. *Nucleic Acids Res* **2017,** 45, D1046–D1053.
59. Singh, R. B.; Mahenderakar, M. D.; Jugran, A. K.; Singh, R. K.; Srivastava, R. K. Assessing genetic diversity and population structure of sugarcane cultivars, progenitor species and genera using microsatellite (SSR) markers. *Gene* **2020,** 753, 144800.
60. Liu, X.; Xu, D.; Hong, Z.; Zhang, N.; Cui, Z. Comparative and Phylogenetic Analysis of the Complete Chloroplast Genome of *Santalum* (Santalaceae). *Forests* **2021**, 12, 1303.
61. Hong, Z.; He, W.; Liu, X.; Tembrock, L. R.; Wu, Z.; Xu, D.; Liao, X. Comparative Analyses of 35 Complete Chloroplast Genomes from the Genus *Dalbergia* (Fabaceae) and the Identification of DNA Barcodes for Tracking Illegal Logging and Counterfeit Rosewood. *Forests* **2022,** 13, 626.
62. Huang, Y.; Li, F.; Chen, K. S. Analysis of diversity and relationships among Chinese orchid cultivars using EST-SSR markers. *Biochemical Systematics and Ecology* **2010,** 38:93–102.
63. Fei, W.; Zhao, W. Z.; Dong, Z. H.; Ma, L. Y.; Li, W. Y.; Li, Z. Y.; Xin, P. Y. Analysis of the Chloroplast Genome Characteristics of 6 Species of *Yucca. Bulletin of Botanical Research* **2023**, 43(01): 109-119.
64. Wu, W. L.; Chung, Y. L.; Kuo, Y. T. Development of SSR Markers in *Phalaenopsis* Orchids, Their Characterization, Cross-Transferability and Application for Identification. *Orchid Biotechnology III* **2017:** 91-107.
65. Lee, Y. F.; Liu, Y. C.; Jheng, C. F.; Lin, J. Y.;Wu, W. L.; Chang, C. C.; Lin, B. Y.; Chen, T. C.; Chen, T. C. Comparative Chloroplast DNA Analysis of *Phalaenopsis* Orchids and Evaluation of cpDNA Markers for Distinguishing Moth Orchids. *Orchid Biotechnology III* **2017:** 61-90.
66. Zheng, S. G.; Hu, Y. D.; Zhao, R. X.; Yan, S.; Zhang, X. Q.; Zhao, T. M.; Chun, Z. Genomewide researches and applications on. *Dendrobium Planta* **2018,** 248, 769–784.
67. Zhao, T. M.; Zheng, S. G.; Hua, Y. D.; Zhao, R. X.; Lia, H. J.; Zhang, X. Q.; Chun, Z. Classification of interspecific and intraspecific species by genome-wide SSR markers on *Dendrobium*(Article). *South African Journal of Botany* **2019:** 136-146.

68. Hua, W. P ; Chen, C. Characterization and SSR identify of the complete chloroplast genome of *Paphiopedilum concolor* (Orchidaceae). *Mitochondrial DNA Part B-Resources* **2019,** Vol.4(No.1): 1074-1076.
69. Fan, J. Z.; Li, X. L.; Li, M. Z.; Bu, Z. Y.; He, J. Z.; Zeng, Y. H. Genomic Characteristics and Phylogenic Analysis of Chloroplast of the Endangered Plant *Paphiopedilum venustum. Chinese Journal of Tropical Crops* **2023**, 44(06): 1097-1105.
70. Li, D. M.; Zhao, C. Y.; Liu, X. F. Complete chloroplast genome sequences of *Kaempferia galanga* and *Kaempferia elegans:* Molecular structures and comparative analysis. *Molecules* **2019,** 24, 474.
71. Mo, Z.; Lou, W.; Chen, Y.; Jia, X.; Zhai, M.; Guo, Z.; Xuan, J. The chloroplast genome of *Carya illinoinensis*: Genome structure, adaptive evolution, and phylogenetic analysis. *Forests* **2020**, 11, 207.
72. Xu, J.; Liu, C.; Song, Y.; Li, M. Comparative Analysis of the Chloroplast Genome for Four *Pennisetum* Species: Molecular Structure and Phylogenetic Relationships. *Front. Genet* **2021**, 12, 687844.
73. Sun, Y.; Zou, P.; Jiang, N.; Fang, Y.; Liu, G. Comparative analysis of the complete chloroplast genomes of nine *Paphiopedilum* species. *Front. Genet* **2022,** 12, 772415.75.
74. Lu, J. J.; Kang, J. Y.; Feng, S. G.; Zhao, H. Y.; Liu, J. J.; Wang, H. Z. Transferability of SSR markers derived from *Dendrobium nobile* expressed sequence tags (ESTs) and their utilizationin *Dendrobium* phylogeny analysis. *Scientia Horticulturae* **2013**, 158: 8–15.
75. Tang, C. Q.; Qiu, Z. X.; Tan, C.; Qian, Y. M.; Chen, X. *Sorbus koehneana* (Rosaceae): Its Complete Chloroplast Genome and Phylogenetic Relationship with *S. unguiculata. Acta Horticulturea Sinica* **2022,** 49 (3): 641–654.
76. Gamisch, A.; Winter, K.; Fischer, G. A.; Peter, C. H. Evolution of crassulacean acid metabolism (CAM) as an escape from ecological niche conservatism in Malagasy *Bulbophyllum* (Orchidaceae). *New Phytologist* **2021,** 231(3): 1236–1248.
77. Hu, A.; Gale, S. W.; Liu, Z. J.; Fischer, G. A.; Saunders, R. M. Diversification slowdown in the *Cirrhopetalum alliance* (*Bulbophyllum*, Orchidaceae): insights from the evolutionary dynamics of crassulacean acid metabolism. *Frontiers in Plant Science* **2022,** 13: 794171.
78. Lin, M.; Hsu, B. Photosynthetic plasticity of *Phalaenopsis* in response to different light environments. *Journal of Plant Physiology* **2004,** 161(11): 1259–1268.
79. Silvera, K.; Santiago, L. S.; Winter, K. Distribution of crassulacean acid metabolism in orchids of Panama: evidence of selection for weak and strong modes. *Functional Plant Biology* **2005**, 32(5): 397–407.
80. Winter, K.; Holtum, J. Facultative crassulacean acid metabolism (CAM) plants: powerful tools for unravelling the functional elements of CAM photosynthesis. *Journal of Experimental Botany* **2014,** 65(13): 3425–3441.
81. Li, J.; Wang, S.; Yu, J.; Wang, L.; Zhou, S. A. Modified CTAB Protocol for Plant DNA Extraction. *Chin. Bull. Bot* **2013,** 48, 72–78.
82. Jin, J. J.; Yu, W. B.; Yang, J. B.; Song, Y.; DePamphilis, C. W.; Yi, T. S.; Li, D. Z. GetOrganelle: A fast and versatile toolkit for accurate de novo assembly of organelle genomes. *Genome Biol* **2020,** 21, 241.
83. Bankevich, A.; Nurk, S.; Antipov, D.; Gurevich, A. A.; Dvorkin, M.; Kulikov, A. S.; Lesin, V. M.; Nikolenko, S. I.; Pham, S.; Prjibelski, A. D.; et al. SPAdes: A new genome assembly algorithm and its applications to single-cell sequencing. *J. Comput. Biol. J. Comput. Mol. Cell Biol* **2012,** 19, 455–477.
84. Wyman, S. K.; Jansen, R. K.; Boore, J. L. Automatic annotation of organellar genomes with DOGMA. *Bioinformatics* **2004,** 20, 3252–3255.
85. Kearse, M.; Moir, R.; Wilson, A.; Stones-Havas, S.; Cheung, M.; Sturrock, S.; Buxton, S.; Cooper, A.; Markowitz, S.; Duran, C.; Thierer, T.; Ashton, B.; Meintjes , P.; Drummond, A. Geneious Basic: An integrated and extendable desktop software platform for the organization and analysis of sequence data. *Bioinformatics* **2012,** 28, 1647–1649.
86. Greiner, S.; Lehwark, P.; Bock, R. OrganellarGenomeDRAW (OGDRAW) version 1.3.1: Expanded toolkit for the graphical visualization of organellar genomes. *Nucleic Acids Res* **2019,** 47, W59–W64.
87. Brudno, M.; Malde, S.; Poliakov, A.; Do, C.B.; Couronne, O.; Dubchak, I.; Batzoglou, S. Glocal alignment: Finding rearrangements during alignment. *Bioinformatics* **2003,** 19 (Suppl. S1), i54–i62.
88. Rissman, A. I.; Mau, B.; Biehl, B. S.; Darling, A. E.; Glasner, J. D.; Perna, N. T. Reordering contigs of draft genomes using the Mauve aligner. *Bioinformatics* **2009,** 25, 2071–2073.
89. Amiryousefi, A.; Hyvonen, J.; Poczai, P. IRscope: An online program to visualize the junction sites of chloroplast genomes. *Bioinformatics* **2018,** 34, 3030–3031.
90. Katoh, K.; Standley, D. M. MAFFT multiple sequence alignment software version 7: Improvements in performance and usability *Mol. Biol. Evol* **2013,** 30, 772–780.92.
91. Rozas, J.; Ferrer-Mata, A.; Sánchez-DelBarrio, J. C.; Guirao-Rico, S.; Librado, P.; Ramos-Onsins, S. E.; Sánchez-Gracia, A. DnaSP 6: DNA Sequence Polymorphism Analysis of Large Data Sets. *Mol. Biol. Evol* **2017,** 34, 3299–3302.
92. Beier, S.; Thiel, T.; Münch, T.; Scholz, U.; Mascher, M. MISA-web: A web server for microsatellite prediction. *Bioinformatics* **2017,** 33, 2583–2585.
93. Kurtz, S.; Choudhuri, J. V.; Ohlebusch, E.; Schleiermacher, C.; Stoye, J.; Giegerich, R. REPuter: The manifold applications of repeat analysis on a genomic scale. *Nucleic Acids Res* **2001,** 29, 4633–4642.

94. Miller, M. A.; Pfeiffer, W.; Schwartz, T. Creating the CIPRES Science Gateway for inference of large phylogenetic trees. In Proceedings of the 2010 Gateway Computing Environments Workshop (GCE), New Orleans, LA, USA, 14 November **2010**; pp. 1–8.
95. Stamatakis, A.; Hoover, P.; Rougemont, J. A rapid bootstrap algorithm for the RAxML Web servers. *Syst. Biol* **2008,** 57, 758–771.
96. Swofford, D. L. Phylogenetic analysis using parsimony (* and other methods). Sinauer, Sunderland, Massachusetts, USA, **2002**.
97. Ronquist, F.; Teslenko, M.; Van Der Mark, P.; Ayres, D. L.; Darling, A.; Höhna, S.; Larget, B.; Liu, L.; Suchard, M. A.; Huelsenbeck, J. P. MrBayes 3.2: Efficient Bayesian phylogenetic inference and model choice across a large model space. *Syst. Biol* **2012,** 61, 539–542.93.